Formation of Nonclassical Ordered Phases of *AB*-Type Multiarm Block Copolymers

Ya Gao, Hanlin Deng, Weihua Li,* and Feng Qiu
State Key Laboratory of Molecular Engineering of Polymers, Collaborative Innovation Center of Polymers and Polymer Composite Materials, Department of Macromolecular Science, Fudan University, Shanghai 200433, China

An-Chang Shi
Department of Physics and Astronomy, McMaster University, Hamilton, Ontario, Canada L8S 4M1
(Received 27 September 2015; revised manuscript received 21 December 2015; published 11 February 2016)

The formation of ordered phases from block copolymers is driven by a delicate balance between the monomer-monomer interaction and chain configurational entropy. The configurational entropy can be regulated by designed chain architecture, resulting in a new entropy-driven mechanism to control the self-assembly of ordered phases from block copolymers. An effective routine to regulate the configurational entropy is to utilize multiarm architecture, in which the entropic contribution to the free energy could be qualitatively controlled by the fraction of bridging configurations. As an illustration of this mechanism, the phase behavior of two *AB*-type multiarm block copolymers, $B_0-(B_i-A_i)_m$ and $(B_1-A_i-B_2)_m$ where the minority *A* blocks form cylindrical or spherical domains, are examined using the self-consistent field theory (SCFT). The SCFT results demonstrate that the packing symmetry of the cylinders or spheres can be controlled by the length of the bridging *B* blocks. Several nonclassical ordered phases, including a novel square array cylinder with $p4mm$ symmetry, are predicted to form from the *AB*-type multiarm block copolymers.

DOI: 10.1103/PhysRevLett.116.068304

The self-assembly of block copolymers has become a topic attracting extensive attention due to its intriguing properties and potential applications [1–5]. The formation of equilibrium ordered phases from the self-assembly of block copolymer is dictated by a number of factors, including interaction parameters between distinct blocks that are usually quantified by the Flory-Huggins parameter χ, the chain length characterized by the number of statistical segments N, the volume fraction of each block, the monomer size and density, as well as the chain topology. Simple *AB* diblock copolymers, whose phase behavior is mainly governed by two parameters, i.e., the product χN and the volume fraction of *A* block f, exhibit a number of ordered morphologies, including the lamellar, hexagonally packed cylindrical, body-centered-cubic (bcc) spherical, bicontinuous gyroid, and $Fddd$ (O^{70}) phases [6,7]. Block copolymer phase behavior depends on other molecular parameters as well. For example, the conformational asymmetry of *A* and *B* blocks could lead to the formation of novel spherical structures such as the complex Frank-Kasper σ phase [8–10].

The formation of different ordered phases from block copolymers is driven by a competition between the monomer-monomer interaction and the chain connectivity. It has been well established that adding more types of blocks will lead to the formation of complex ordered phases [4]. For example, an *ABC* triblock copolymer is obtained by adding one *C* block onto the *AB* diblock copolymer. It has been shown that *ABC* triblock copolymers can exhibit a much richer phase behavior than the *AB* diblock, largely due to the significantly enlarged parameter space [11–13]. Moreover, the topological structure, e.g., linear versus star, further regulates the self-assembly behavior of *ABC* triblock copolymers [14–19]. The chain topology also plays an important role for bicomponent block copolymers. It has been shown that the perforated lamellar [20], spherical phase with the *A*15 lattice [21–24], and Frank-Kasper σ phase [8–10], become stable in *AB*-type comb or branching copolymers. A further example is found in *ABC* multiblock terpolymers. In these terpolymers the topology becomes a critical factor affecting the formation of equilibrium morphology. For example, Li and co-workers have demonstrated that designed $B_1AB_2CB_3$ terpolymers can be engineered to form various binary mesocrystals with varying coordination numbers (CNs) by changing the relative lengths of the middle and terminal *B* blocks [25,26].

It is straightforward to alter the monomer-monomer interaction by introducing chemically different blocks, electrostatic and hydrogen-bonding interactions into the system. On the other hand, controlling the entropic contribution to the self-assembling process is less straightforward. It has been argued that the introduction of comblike or branch architecture in *AB*-type block copolymers could provide a method to alter the entropic contributions, resulting in ordered phases not available in linear diblock copolymers [20]. Based on this argument we propose that utilizing chain topology to regulate the entropic contributions could provide an effective method for the engineering

of ordered phases. In this work, we demonstrate that the topology of block copolymer can indeed be used to control the formation of ordered phases.

One of the main motivations for the topological design is to regulate the configurational entropy, such as the number of possible configurational paths of multiblock terpolymer chain going through lamella-within-lamella hierarchical structures [27] and the ratio of looping and bridging configurations [28]. Although the concept of bridging configuration has been introduced and discussed by experimenters [29] and theorists [30] previously, its effect on the equilibrium morphology is rarely explored. In the $B_1AB_2CB_3$ terpolymers, "bridge" is naturally formed due to the constraint of A and C domains on the minority A and C blocks. This constraint is absent in AB-type copolymers [25]. However, as mentioned before, a certain fraction of bridging configurations is obtained in ABA triblock copolymers due to the maximization of configurational entropy [31]. More importantly, the bridging fraction can be significantly enhanced in multiarm copolymers because the combinatorial entropy increases with the number of arms and therefore the configurational entropy could be more dominant over other free-energy contributions [28]. Regulating the configurational entropy offers the possibility to tune the packing symmetry of cylinders or spheres in AB-type copolymers. Compared with the tuning mechanism in the previous $B_1AB_2CB_3$ system, one more factor of adjustable relative length of bridges is required.

In order to regulate the configurational entropy, we design two AB-type multiarm block copolymers, in which m identical arms join together to form a star topology (Fig. 1). This special architecture enables the construction of effective bridges by partitioning multiple arms into different neighboring domains due to two driving forces, the combinatorial entropy and the conformational asymmetry. The latter arises from the fact that localizing multiple branches into a single minority domain results in an excessive packing frustration [24]. In the first molecule, M_1, consisting of one block of B homopolymer joined to m $(B_i - A_i)$ diblocks at a common junction point, the B_i blocks act as the bridges, and their length can be varied by modifying the length of the tail B_0 block while keeping the total B composition unchanged.

For the linear AB diblock copolymer with fixed χN, the competition of the stretching energy and the interfacial energy is mainly dictated by the compositional parameter f. In contrast, the competition between these two factors in M_1 with constant χN and f can also be regulated by adjusting the length of the bridging blocks. Short bridging blocks favor close interface separation between domains to avoid excessive stretching. On the other hand, the closer arrangement of domains leads to smaller domains and thus to higher interfacial energy. An effective way to mitigate this competition is to rearrange the microdomains onto new crystal lattices with a more adaptive coordination

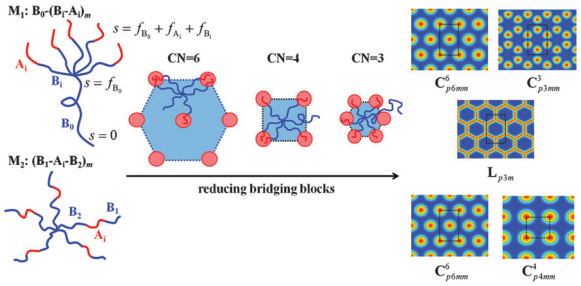

FIG. 1. Left: schematic plot of the architectures of the two designed AB-type multiblock copolymers, M_1 and M_2. A and B blocks are drawn in red and blue colors, respectively. Center: illustrative plot of chain configurations in three typical cylindrical morphologies with different coordination numbers demonstrating the formation of bridges among neighboring domains and their impact on the domain arrangement (i.e., packing lattice). Right: density profiles of the stable morphologies self-assembled from the two block copolymers, including the classical phase of hexagonal cylinders (denoted as C^6_{p6mm}, where the subscript and superscript indicate the plane symmetry and coordination number, respectively) and three nonclassical phases of square array of cylinders (similarly denoted as C^4_{p4mm}), graphenelike cylinders (C^3_{p3mm}), and honeycomblike network phase (L_{p3m}). More candidate phases are listed in Fig. S1 [32].

environment [25]. It has been proposed that a crystal lattice with lower CN tends to have a closer interface separation of domains that benefits releasing the stretching of the bridging blocks. As the length of the bridges is shortened, the cylindrical or spherical morphology transfers from the crystal lattice of high CN to that of low CN. The energy benefiting from the reduced stretching of the bridging blocks compensates the energy cost due to the higher noncircularity and nonsphericity of domains on a crystal lattice with lower CN [9]. Therefore, the number of arms and the length of the bridging B blocks can be used as a controlling parameter for the formation of different ordered phases. This mechanism of regulating configuration entropy via multiarm block copolymers is illustrated schematically in Fig. 1.

Based on the proposed design principle of bridging B blocks with adjustable length, we design a second architecture, denoted as M_2, where the homopolymer B block is transformed into m identical B blocks added to the end of each A_i block (Fig. 1). Bridge motifs are constructed in a similar way, where the length of the bridge is tuned by varying the location of the A_i block within each arm. In order to verify the proposed entropy-driven mechanism, the phase diagrams of varying block ratios for fixed χN are determined using the pseudospectral method of SCFT [34–36]. Details of the SCFT formulation are provided in the Supplemental Material [32]. Transitions between various ordered phases with respect to the relative lengths of B blocks with fixed total B compositions are identified. The main results for M_1 and M_2 are summarized in the 2D

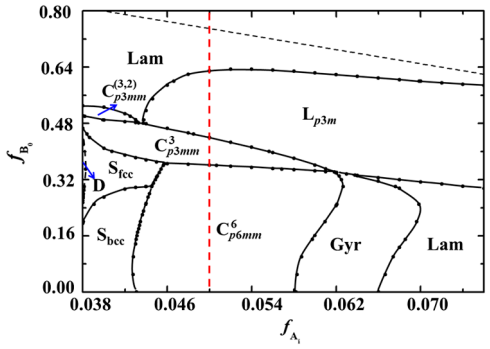

FIG. 2. Phase diagram of molecule M_1 in the $f_{A_i} - f_{B_0}$ plane with $m = 5$ and $\chi N = 100$. The red dashed line indicates the phase path of $f_{A_i} = 0.05$.

cross-sectional phase diagrams of Figs. 2 and 3, respectively. It is noted that the SCFT is a mean-field theory; thus, fluctuation effects are ignored. It is known that fluctuation effects can be important in the weak-segregation regime [37]. On the other hand, for block copolymers in the intermediate to strong segregation regime, the SCFT provides an accurate description of their phase behavior.

As we expect to adjust the coordination environment via tailoring the bridge motifs, we first examine the configurational change as the length of bridging blocks varies. As an example, we show in Fig. 4 the density distribution of the junction point of M_1 within the unit cell of the C^4_{p4mm} phase for a set of f_{B_0} values. The results show that the bridge motifs undergo a notable transition as f_{B_0} increases, i.e., that the bridging blocks are shortened. When f_{B_0} is less than 0.2, the junction point is distributed mainly in the central region of the cell, indicating that the A_i blocks are partitioned evenly into the surrounding four domains. This greatly increases the combinatorial entropy of the A_i blocks and also favors reducing their packing frustration. As f_{B_0} increases from 0.2 to 0.4, the bridging blocks begin to experience severe stretching (Fig. S3 [32]). Driven by the effort to alleviate the degree of stretching, the junction point

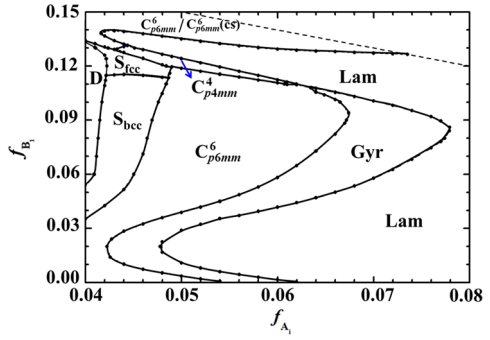

FIG. 3. Phase diagram of molecule M_2 in the $f_{A_i} - f_{B_1}$ plane with $m = 5$ and $\chi N = 140$. In the upper region of the diagram, the C^6_{p6mm} phase transforms continuously into a core-shell cylinder phase denoted as C^6_{p6mm}(cs), and thereby no boundary is plotted.

gradually moves toward the edge of the cell. Under this condition, the bridges tend to mainly partition into the two nearest domains. Finally, as f_{B_0} further increases up to 0.5, the bridges ultimately degenerate into loops surrounding a single domain.

The calculated variation of the bridge motifs sheds light on the entropy-driven transition mechanism between distinct cylindrical phases. The transition of bridge motifs in other 2D phases is similar to that in the C^4_{p4mm} phase, except that the boundaries are shifted (Fig. S4 [32]). It is also found that the bridges formed in molecule M_2 possess a similar transition process that will be shown to play a crucial role on stabilizing the desired C^4_{p4mm} phase.

To understand the entropy-driven transition mechanism of equilibrium cylindrical phases of M_1 due to adjustable fraction of bridging configurations, we discuss the typical phase path of $f_{A_i} = 0.05$, which goes from the classical cylindrical phase, through two new interesting phases of C^3_{p3mm} and L_{p3m}, to the classical lamellar phase as f_{B_0} increases. As a delicate balance between the interfacial energy and the stretching energy determines the stable phase, we elucidate the underlying mechanism of the phase transitions by analyzing the two contributions of free energy (Fig. S5 [32]).

When f_{B_0} of M_1 is small, the hexagonal phase of C^6_{p6mm} is generally preferred among the cylindrical phases due to its superior capacity to simultaneously minimize the interfacial area and packing frustration [Fig. S5(a) [32]] [23]. On the other hand, the hexagonal phase with the largest CN among the cylindrical phases possesses the least neighboring A domains (i.e., three) for the A arms of one chain to be partitioned (Fig. 1). When f_{B_0} is increased at fixed f_{A_i}, A domains tend to pack more closely in order to reduce the loss of configurations. Because of fixed A-B

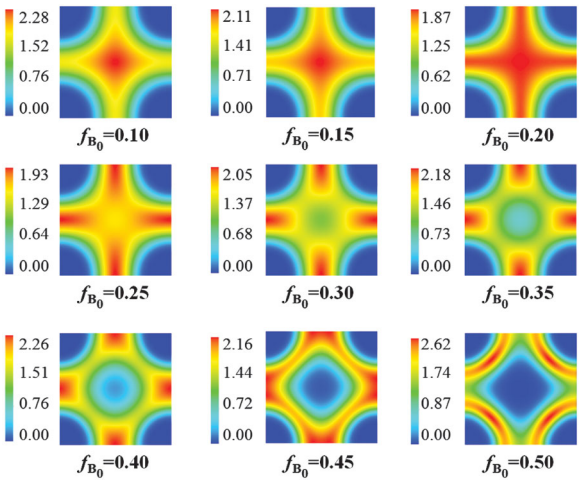

FIG. 4. Density profiles of the junction point of M_1 in the C^4_{p4mm} phase for various f_{B_0} with $f_{A_i} = 0.05$. The density distribution along the middle line of the cell, i.e., $y = L_y/2$, is plotted in Fig. S2 [32].

compositions, reduced domain distance leads to shrunk domains and thus to higher interfacial energy. A lower-coordinated packing lattice with more swollen domains is preferred (Fig. S6 [32]). Accordingly, the phase sequence in the order of favorable interfacial energy as f_{B_0} increases or f_{B_i} decreases is C^6_{p6mm}, C^4_{p4mm}, and C^3_{p3mm}.

Based on the SCFT results, it can be concluded that shorter bridging B blocks make the copolymers flexible and responsive to the coordination environment, thereby resulting in the possible formation of the cylindrical phases with lower CN. For example, the C^3_{p3mm} phase becomes stable only when f_{B_0} is larger than 0.28. Note that lower-coordinated packing is also beneficial to the accommodation of long B_0 blocks as their configurations are disturbed by surrounding A domains and are effectively compressed in the matrix. Entropic loss due to this compression is diminished in the phase of lower CN with more accessible space [Fig. S5(c) [32]]. All these factors operate synergistically to decrease CN when f_{B_0} is increased. Consequently, the stable phase changes from C^6_{p6mm} directly to C^3_{p3mm}, resulting in the absence of C^4_{p4mm} in the phase diagram.

As f_{B_0} is further increased above 0.45, another nonclassical phase, L_{p3m}, emerges and occupies a considerable region in the phase diagram. In this structure the A component forms a threefold continuous network that divides the B matrix into separate hexagonal domains. This honeycomblike phase has been observed in another AB-type block copolymer, i.e., linear-dendrimer copolymers [38]. The stabilization of L_{p3m} phase is accompanied by an abrupt change in both entropic and interfacial energies. The network A domains enclosing each hexagonal B domain impose a strong constraint as complete confinement on the long tail B_0 block [38], resulting in a great loss of its configurational entropy. This entropic loss is more pronounced than those in the cylindrical phases [Fig. S5(c) [32]]. On the other hand, merging isolated domains into continuous lamellalike domains efficiently reduces the interfacial area. This significant drop in interfacial energy compensates the entropic loss and yields a large region of L_{p3m} in the phase diagram.

Eventually, the lamellar phase becomes stable as f_{B_0} is increased to around $f_{B_0} = 0.64$. The higher interfacial energy of the lamellar phase compared to L_{p3m} in Fig. S5(b) [32] is confirmed by a comparison of the density distribution of the A component in the two phases (Fig. S7 [32]). Severe intervening A-B interfaces, indicating strong A-B interaction throughout the A domains, give rise to higher interfacial energy in the lamellar phase. On the contrary, the lamellar phase suffers less loss of entropy, because the constraint on the configuration of the long tail B_0 block consists in only one dimension normal to the A-B interface, whereas in L_{p3m} it is imposed on two dimensions. Even though the 120° corners in L_{p3m} can provide negative curvature to benefit partitioning multiple arms, the entropic factor in respect of B_0 becomes more dominant as the tail block is elongated, and ultimately leads to the stable lamellar phase.

The study of the first macromolecule M_1 demonstrates the successful modulation of phase transitions by regulating configurational entropy for fixed χN and f. Since the highly desired C^4_{p4mm} phase is absent in the phase diagram of M_1, an alternative molecular architecture is examined. As the formation of lower-coordinated phases in M_1 is driven by both the transition of bridge motifs and the configurational constraint on the tail block simultaneously, we devise another molecular architecture with the aim to screen the latter factor, and thus to slow down the decreasing tendency of CN and enable the formation of C^4_{p4mm}. The molecule M_2 is a $(B_1 - A_i - B_2)$-triblock jointed star copolymer in which the inner B_2 blocks act as the bridging blocks like B_i in M_1. However, the difference consists in that each portion of reduction in f_{B_2} brings about an equivalent increment in f_{B_1}, while in M_1, each portion of reduction in f_{B_1} results in an increment by m times in f_{B_0}. It is also worth noting that the molecular architecture of M_2 has a simpler topology and thus is more accessible in synthesis, but without losing the key element of bridge motifs.

As shown in Fig. 3, a sizable region of C^4_{p4mm} is present in the upper-left region of the phase diagram, and a transition from C^6_{p6mm} to C^4_{p4mm} as f_{B_1} increases is observed as expected. To show the effect of configurational entropy on this phase transition, we compare the distributions of the junction point of M_2 in the C^4_{p4mm} and C^6_{p6mm} phases in the region where C^4_{p4mm} is stable. As shown explicitly in Fig. S8 [32], the proportion of bridging configurations is considerable in C^4_{p4mm} while most of them have degenerated in C^6_{p6mm}. This is well consistent with the proposed entropy-driven mechanism.

Similar to the phase transitions between the cylindrical phases, the configurational entropy also has a significant effect on the transition between the spherical phases of S_{bcc} and S_{fcc} in the left region of the phase diagram where f_{A_i} is relatively small. The stable spherical phase of AB diblock copolymer is mainly S_{bcc}, except for a tiny region of S_{fcc} phase at the vicinity of the order-disorder transition boundary [20]. Obviously, in the current systems the transition of the spherical phases is not simply driven by the variation of segregation degree. Instead, the mechanism is similar as that in the cylindrical phases. Decreasing the length of bridging blocks permits a larger distortion of domains away from sphericity, which is in accordance with the sphericity argument because the isoperimetric quotient, $\mathrm{IQ} = 0.7534$ of S_{bcc} is larger than $\mathrm{IQ} = 0.7405$ of S_{fcc} [9]. Although nonclassical spherical phases are not formed in the current system, they could be stabilized in other

bicomponent copolymers designed according to the principle of regulating the configurational entropy.

Of the new morphologies exhibited by the current *AB* multiarm copolymers, the square array of cylinders is of special interest due to its potential application in nanolithography [39]. While chemical patterns with hexagonal symmetry act as excellent templates for the assembly process [40], the square lattice of microdomains is generally more consistent with the industry-standard coordinate system, thus more desirable in microelectronic applications. Even though ordered square arrays have been obtained via templated self-assembly of triblock copolymers and supramolecular block copolymers [39,41–43], long-range and defect-free pattern remains a challenge for *AB*-type block copolymers.

Square cylindrical phase has been observed experimentally in the self-assembly of copolymeric dendrimers and supramolecular dendronized polymers [44,45]. A later theoretical study implies that polymeric architectures with a long handle are essential for stabilizing the square phase, and a large number of tines helps expand its stability region [46]. These previous studies provide great inspiration to the search of square cylindrical phases. Nevertheless, a general mechanism is lacking to rationalize the formation of the square phase, without which it is unlikely to realize the goal of topological design for more desired phases.

In the current work, we propose an entropy-driven mechanism for the formation of nonclassical equilibrium morphologies from the self-assembly of *AB*-type block copolymers. It should be pointed out that in our systems of *AB*-type multiblock copolymers, the formation of bridge motifs due to maximizing the configurational entropy by partitioning multiple arms into different neighboring domains is in contrast to that of the bridges constrained between *A* and *C* domains in the binary crystalline phases of *ABC*-type multiblock terpolymers. However, these two designed block copolymer architectures exhibit a similar impact on the transitions between phases with various CNs. Therefore, the current work further enriches the design principle of topological architecture of block copolymers for the fabrication of desired structures, which was originally demonstrated via the self-assembly of $B_1AB_2CB_3$ multiblock terpolymers in our previous work.

This work was supported by the National Natural Science Foundation of China (Grants No. 21322407 and No. 21574026). A.-C. Shi acknowledges the support from the Natural Science and Engineering Research Council (NSERC) of Canada.

Y. G. and H. D. contributed equally to this work.

*weihuali@fudan.edu.cn

[1] F. S. Bates and G. H. Fredrickson, Annu. Rev. Phys. Chem. **41**, 525 (1990).
[2] S. B. Darling, Prog. Polym. Sci. **32**, 1152 (2007).
[3] I. W. Hamley, Prog. Polym. Sci. **34**, 1161 (2009).
[4] F. S. Bates, M. A. Hillmyer, T. P. Lodge, C. M. Bates, K. T. Delaney, and G. H. Fredrickson, Science **336**, 434 (2012).
[5] W. H. Li and M. Müller, Annu. Rev. Chem. Biomol. Eng. **6**, 187 (2015).
[6] M. W. Matsen and M. Schick, Phys. Rev. Lett. **72**, 2660 (1994).
[7] C. A. Tyler and D. C. Morse, Phys. Rev. Lett. **94**, 208302 (2005).
[8] S. Lee, M. J. Bluemle, and F. S. Bates, Science **330**, 349 (2010).
[9] S. Lee, C. Leighton, and F. S. Bates, Proc. Natl. Acad. Sci. U.S.A. **111**, 17723 (2014).
[10] N. Xie, W. H. Li, F. Qiu, and A. C. Shi, ACS Macro Lett. **3**, 906 (2014).
[11] F. S. Bates and G. H. Fredrickson, Phys. Today **52**, No. 02, 32 (1999).
[12] Z. Guo, G. Zhang, F. Qiu, H. Zhang, Y. Yang, and A. C. Shi, Phys. Rev. Lett. **101**, 028301 (2008).
[13] W. Xu, K. Jiang, P. Zhang, and A. C. Shi, J. Phys. Chem. B **117**, 5296 (2013).
[14] T. Gemma, A. Hatano, and T. Dotera, Macromolecules **35**, 3225 (2002).
[15] C. A. Tylor, J. Qin, F. S. Bates, and D. C. Morse, Macromolecules **40**, 4654 (2007).
[16] Y. Matsushita, Macromolecules **40**, 771 (2007).
[17] W. H. Li, Y. C. Xu, G. J. Zhang, F. Qiu, Y. L. Yang, and A. C. Shi, J. Chem. Phys. **133**, 064904 (2010).
[18] W. H. Li, F. Qiu, and A. C. Shi, Macromolecules **45**, 503 (2012).
[19] M. J. Liu, W. H. Li, F. Qiu, and A. C. Shi, Macromolecules **45**, 9522 (2012).
[20] M. W. Matsen, Macromolecules **45**, 2161 (2012).
[21] V. S. K. Balagurusamy, G. Ungar, V. Percec, and G. Johansson, J. Am. Chem. Soc. **119**, 1539 (1997).
[22] B. K. Cho, A. Jain, S. M. Gruner, and U. Wiesner, Science **305**, 1598 (2004).
[23] G. M. Grason, B. A. DiDonna, and R. D. Kamien, Phys. Rev. Lett. **91**, 058304 (2003).
[24] G. M. Grason and R. D. Kamien, Macromolecules **37**, 7371 (2004).
[25] N. Xie, M. J. Liu, H. L. Deng, W. H. Li, F. Qiu, and A. C. Shi, J. Am. Chem. Soc. **136**, 2974 (2014).
[26] M. J. Liu, B. K. Xia, W. H. Li, F. Qiu, and A. C. Shi, Macromolecules **48**, 3386 (2015).
[27] W. H. Li and A. C. Shi, Macromolecules **42**, 811 (2009).
[28] Y. C. Xu, W. H. Li, F. Qiu, and Z. Q. Lin, Nanoscale **6**, 6844 (2014).
[29] M. D. Gehlsen, K. Almdal, and F. S. Bates, Macromolecules **25**, 939 (1992).
[30] M. W. Matsen and R. B. Thompson, J. Chem. Phys. **111**, 7139 (1999).
[31] S. Woloszczuk, K. P. Mineart, R. J. Spontak, and M. Banaszak, Phys. Rev. E **91**, 010601(R) (2015).
[32] See Supplemental Material at http://link.aps.org/supplemental/10.1103/PhysRevLett.116.068304 which includes Ref. [33], for details of the theoretical methods, all considered phases, and some supplemental data about the bridge motifs as well as the free-energy comparisons.
[33] R. B. Thompson, K. Ø. Rasmussen, and T. Lookman, J. Chem. Phys. **120**, 31 (2004).

[34] K. Ø. Rasmussen and G. Kalosakas, J. Polym. Sci., Part B: Polym. Phys. **40**, 1777 (2002).
[35] G. Tzeremes, K. Ø. Rasmussen, T. Lookman, and A. Saxena, Phys. Rev. E **65**, 041806 (2002).
[36] G. H. Fredrickson, *The Equilibrium Theory of Inhomogeneous Polymers* (Oxford Univ. Press, Oxford, 2006).
[37] G. H. Fredrickson and E. Helfand, J. Chem. Phys. **87**, 697 (1987).
[38] G. T. Pickett, Macromolecules **35**, 1896 (2002).
[39] C. Tang, E. M. Lennon, G. H. Fredrickson, E. J. Kramer, and C. J. Hawker, Science **322**, 429 (2008).
[40] R. Ruiz, H. Kang, F. A. Detcheverry, E. Dobisz, D. S. Kercher, T. R. Albrecht, J. J. de Pablo, and P. F. Nealey, Science **321**, 936 (2008).
[41] H. L. Chen, J. S. Lu, C. H. Yu, C. L. Yeh, U. S. Jeng, and W. C. Chen, Macromolecules **40**, 3271 (2007).
[42] J. Xu, T. P. Russell, B. M. Ocko, and A. Checco, Soft Matter **7**, 3915 (2011).
[43] J. G. Son, J. Gwyther, J. B. Chang, K. K. Berggren, I. Manners, and C. A. Ross, Nano Lett. **11**, 2849 (2011).
[44] R. Martin-Rapun, M. Marcos, A. Omenat, J. Barbera, P. Romero, and J. L. Serrano, J. Am. Chem. Soc. **127**, 7397 (2005).
[45] N. Canilho, E. Kasemi, A. D. Schiluter, and R. Mezzenga, Macromolecules **40**, 2822 (2007).
[46] W. B. Lee, R. Elliott, R. Mezzenga, and G. H. Fredrickson, Macromolecules **42**, 849 (2009).